An active bubble trap and debubbler for microfluidic systems†

Alison M. Skelley[a,b] and Joel Voldman[a,b,c]

Received 29th April 2008, Accepted 16th July 2008
First published as an Advance Article on the web 28th August 2008
DOI: 10.1039/b807037g

We present a novel, fully integrated microfluidic bubble trap and debubbler. The 2-layer structure, based on a PDMS valve design, utilizes a featured membrane to stop bubble progression through the device. A pneumatic chamber directly above the trap is evacuated, and the bubble is pulled out through the gas-permeable PDMS membrane. Normal device operation, including continuous flow at atmospheric pressure, is maintained during the entire trapping and debubbling process. We present a range of trap sizes, from 2 to 10 mm diameter, and can trap and remove bubbles up to 25 μL in under 3 h.

Introduction

Unwanted bubbles inadvertently introduced into a microfluidic system can significantly and negatively affect device operation and experimental outcome. A great deal of care is required to operate and fill these devices under bubble-free conditions. This is especially true for microfluidic perfusion culture systems, which typically require sterilization and pre-conditioning of the surface prior to cell seeding, time to allow for cell attachment, and then take several days to observe the growth rate and cell morphologies.[1–3] Bubbles can form at the connection between the device and tubing or can be introduced when unplugging connections to transfer the device between the microscope and incubator. If the bubble makes it into the growth area it completely fouls the experiment: the bubbles are cytotoxic to the cells and will rupture their cell membranes.[4] As such, microfluidic systems are extremely sensitive to even a small bubble introduced into the device at any time during cell culture.

One solution to mitigate bubble-based device failure is to integrate microfluidic features to prevent bubbles from entering critical areas of a device. There are, in general, two different approaches: trapping *versus* debubbling. A bubble trap is a structure integrated into the flow system that halts further progress of a bubble through a device. Eddington demonstrated a simple, easily implemented bubble trap by making a chamber at the connection point between external tubing and their device.[4] This approach has the advantage that device operation is maintained while the bubbles are trapped. However, because the bubble trap does not remove bubbles from the system, if the bubble trap completely fills with bubbles, then any additional bubbles would be sent through the system and lead to device failure. The alternative, demonstrated by Kang *et al.*, is to actively remove the bubbles from the system.[5] This method relies upon the gas permeability of PDMS and uses positive pressure to force bubbles out of the channel. The advantage here is that the bubbles are removed from the system, but to do so the device has to be sealed, flow stopped, and the device pressurized to force bubbles out. For a microfluidic perfusion system, this means that the media supply to the cells is stopped, pausing the experiment, altering the environment and possibly leading to nutritional deficiencies, and the cells are then subjected to higher than normal pressures while the bubble is removed.

Instead, we present a bubble trap and debubbler that has both the ability to trap a bubble while maintaining device operation, and to then remove this bubble from the system, still under normal device operation. The device is modeled after the valves demonstrated by Irimia *et al.*, consisting of a 2-layer PDMS device containing fluidic and pneumatic channels.[6] In our design the bubble is securely trapped in a bubble trap region defined by a ring-shaped corral, and the applied vacuum, required to keep the trap open, also serves to pull the gas in the bubble out through the permeable PDMS membrane. We demonstrate trapping of bubbles from 2 to 25 μL, and removal of the largest of these bubbles in under 3 h while maintaining steady, uninterrupted flow.

Experimental

Fabrication of the bubble trap

The bubble trap is composed of two layers of PDMS, both featured, that are bonded together. First, 3-D AutoCad drawings were used to generate 3-D plastic molds (Fineline, NC). The molds were silanized for 24 h in a vacuum chamber with (tridecafluoro-1,2,2-tetrahydrooctyl)-1-tricholorosilane (T2492-KG,United Chemical Technologies, PA). The pneumatic mold contained the inverse of the 150 μm tall displacement chambers surrounded by a 3 mm tall lip (Fig. 1). PDMS was poured to the overflow point, setting the overall thickness of the pneumatic layer at 3 mm. The fluidic mold contained all fluidic channels (250 μm tall) and circular trapping ridges (400 μm

[a]*Research Laboratory of Electronics, Massachusetts Institute of Technology, Cambridge, MA, 02139, USA*
[b]*Microsystems Technology Laboratory, Massachusetts Institute of Technology, Cambridge, MA, 02139, USA*
[c]*Electrical Engineering and Computer Science Department, Massachusetts Institute of Technology, Room 36-824, 77 Massachusetts Ave, Cambridge, MA, 02139, USA. E-mail: voldman@mit.edu; Fax: +1 617 258 5846; Tel: +1 617 253 2094*

† Electronic supplementary information (ESI) available: Video file and description. See DOI: 10.1039/b807037g

This journal is © The Royal Society of Chemistry 2008

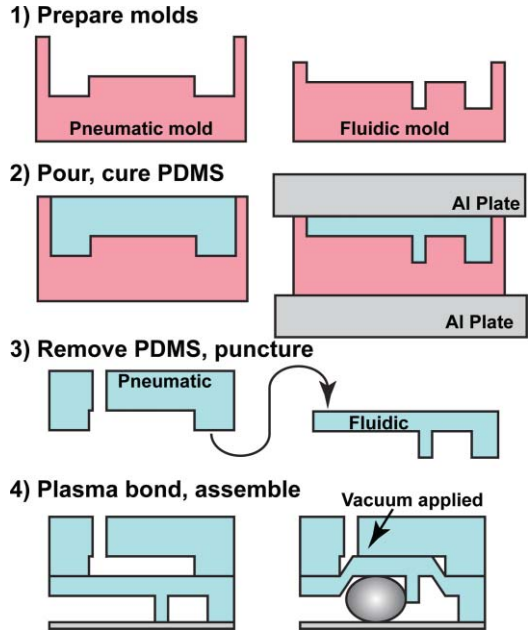

Fig. 1 Schematic of the device construction and assembly. The two layers of PDMS are cured separately, connections to the pneumatic layer are punctured, then the layers are plasma bonded together. A glass or polystyrene slide is used as the bottom piece.

horizontal width). Support pillars (500 μm tall) were placed regularly near channel features and around the perimeter. PDMS was poured on the mold, a transparency film was laid on top, and then the entire assembly was placed between 2 aluminium plates, clamped, and cured for 24 h at 65 °C. This set the overall thickness of the fluidic layer at 500 μm, and the thickness of the actuating membrane at 250 μm (Fig. 1).

After curing, the PDMS layers were removed from the molds. Pneumatic connections were punctured using thin-walled stainless steel tubing (0.07″ od × 0.0653″ id, Small Parts Inc.). The featured side (bottom) of the pneumatic layer and blank (top) side of the fluidic layer were plasma cleaned, hand aligned, and bonded together. The device was left to bond for 1 h at 65 °C. Next, fluidic connections were punctured through both layers. The underside of the assembled PDMS piece (containing fluidic features) and a blank glass slide were plasma cleaned, aligned and bonded together, then left to adhere again at 65 °C for 1 h. Alternatively, the device was reversibly bonded to a glass or polystyrene slide.

Device assembly

The PDMS trap was first connected to a vacuum source (house vacuum, –97 kPa relative to atmospheric pressure). The fluidic channel was filled with 80% EtOH/ddH_2O to ensure a bubble-free initial fill. The inlet of the device was connected to a fluid reservoir (food coloring in PBS) *via* peek tubing (0.020″ or 0.008″ id) and the outlet was connected to a syringe pump set to withdraw at 0.1 mL h^{-1}.

Bubble generation and measurement

We generated bubbles by removing the peek tubing from the fluidic reservoir and pulling a bubble into the tubing. The bubble volume was calculated from the length of the bubble and the known internal diameter of the tubing. Once we obtained the desired volume, the tubing was put back in the fluid reservoir (or one containing PBS of a different color), and the bubble traversed through the tubing and into the trap, propelled by the syringe pump. The time the bubble entered the trap was taken as $t = 0$, and we visually determined the time when the bubble was removed.

Results

Microfluidic cell culture systems often operate over multiple days, and during that time continuous, bubble-free flow must be applied to the cells. Bubble introduction (often from the connection point between PEEK tubing and PDMS) is a common occurrence, and once the bubble enters the culture area it destroys the cells. We desired an active bubble trap that would (1) be easily fabricated and directly incorporated into our existing designs such that it was placed immediately before the cell culture area, (2) would prevent the bubbles from moving through the system towards the cells, and (3) would remove bubbles from the system while operating the device normally.

We designed different ridge geometries for capturing the entering bubbles (Fig. 2(A)), including split semi-circle, semi-circle, full circle and full circle with funnel designs (X, Y, Z and V respectively); all effectively trapped and debubbled solutions, but the circular funnel design (Fig. 2(A) and (B)) operated most reproducibly over a range of bubble sizes. The ridge hanging down from the membrane provided an obstacle for entering bubbles, causing the bubbles to expand laterally instead of squeezing underneath. These debubbler geometries were sized to fit upstream of a cell culture device, therefore the channel height was set at 250 μm, the same height as our existing cell culture devices. Different circular ridge widths were tested; 400 μm wide ridges were easily and reproducibly fabricated from the molds, and did not collapse if the pneumatic chamber was pressurized (~ 2 : 1 thickness to height ratio). The height of the pneumatic chamber was set at 150 μm; taller chambers resulted in the membrane stretching too much to deflect, either tearing (especially when using thin membranes) or pulling the fluidic channels away from the glass and generating leaks between valves and/or channels. Finally, the thickness of the membrane was set at 250 μm; thinner membranes were difficult to cure and handle, while thicker membranes, though fully functional, would presumably result in slower debubbling times. We observed that these dimensions resulted in the membrane contacting the roof of the chamber during valve/trap actuation.

We tested the trap at 0.1 mL h^{-1}, typical flow rates for our cell culture devices.[1,3] Bubbles were generated in the tubing and then driven through the trap. For all trap sizes we observed four modes of operation: first, a minimum bubble size (~ 1 μL) was required in order to move into the trap, otherwise the bubble remained at the connection point between the peek tubing and the PDMS device. Second, a larger bubble, upon entering the device, was funneled into the center of the trap, as shown in Fig. 3 (45 s) and ESI Video 1.† The bubbles were reproducibly corralled into the circular ridge. Once the tail end of the bubble was pushed into the entrance a fluidic connection was made around the bubble and under the bottom of the circular ridge, therefore the

 This journal is © The Royal Society of Chemistry 2008

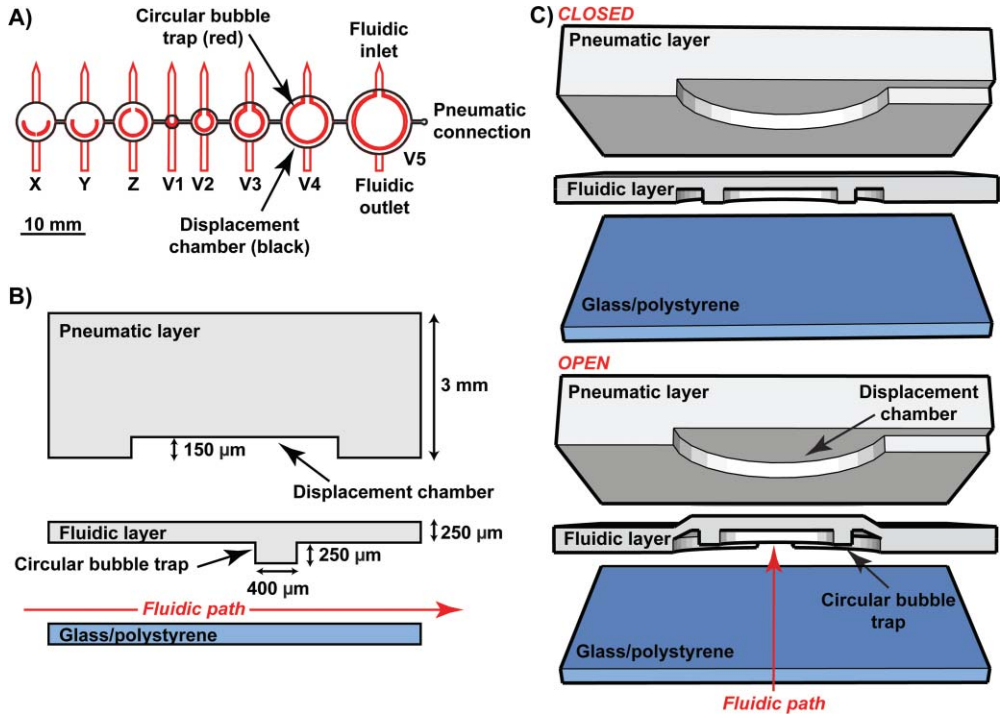

Fig. 2 Top, side and 3-D views of the bubble traps. (A) Top view of the test structures, shown to scale. The trap consists of pneumatic and fluidic layers that are aligned and bonded together. The pnematic layer contains the displacement chamber, and the fluidic layer contains the inlet, outlet and circular bubble trap. (B) Side view of the trap geometry with relevant dimensions. (C) 3-D view showing the two layers of PDMS. A vacuum in the displacement chamber pulls the circular trap up, opening a fluidic connection between the inlet and outlet of the channel. The bubble is trapped by the circular ridge of PDMS that extends down into the channel.

bubble remained stationary. This fluidic connection was stably maintained as illustrated by the changeover between red and blue solutions (Fig. 3). Third, if the bubble volume exceeded the volume of the internal circular area the bubble would break underneath the ridge (on only one side) and expand into the channel on the outside of the trap (not shown). This position still trapped the bubble and provided uninterrupted fluid flow. Finally, if the bubble was too large to fit inside the circular ridge, it would first break underneath the ridge, fill one side of the outer channel, and then push through the output, causing device failure. For all trap sizes shown in Fig. 2 we ran a series of bubble volumes through the device. If the bubble was trapped we determined how long it took for the bubble to be removed from the system, and then we also determined the maximum bubble volume that could be trapped without disrupting flow through the outlet channel.

Shown in Fig. 4 are the debubbling times for a variety of bubble volumes run in traps ranging from 2 to 10 mm in diameter. The debubbling time is independent of the bubble trap diameter but is linearly dependent upon the bubble volume, suggesting that regardless of trap geometry the bubbles are exposed to vacuum across the same surface area. This result corresponds with our observation that the membrane contacts the roof of the pneumatic chamber during actuation; as a result vacuum is likely only presented to the membrane around the edges of the chamber (see Fig. 1). Due to the trap geometry, the bubbles are funneled into the center of the valve (Fig. 2 and 3), so the only region where the bubbles are exposed to the vacuum is at the trap entrance, and this geometry is common across all valves.

We also determined debubbling times for bubbles too large to be contained by the circular ridge, but still small enough to be immobilized (Fig. 4, red dashed circles). In some cases the bubble would extend beyond the circular ridge and lodge against the far edge of the valve; in these instances the debubbling times were smaller than expected, consistent with our assumption of vacuum only being applied at the edges of the trap. We also observed some cases where large bubbles would just pierce the circular ridge, and the back end of the bubble would lodge further into the trap than typically observed. In this case we recorded larger debubbling times than expected, presumably because the bubble was exposed to vacuum over a smaller area.

With our largest debubbler we were able to trap bubbles up to 25 µL in volume, and these bubbles were removed from the system in under 3 h. For comparison, we also trapped bubbles without applying any vacuum (valve permanently bonded open) and monitored the bubble volume; after 24 h no change in bubble volume was observed although there was still continuous flow through the system.

Fig. 5 demonstrates the relationship between trap diameter and maximum bubble volume captured before disruption of fluid flow. The volume of the full open trap was calculated as a 400 µm tall cylindrical volume, ignoring contributions from the circular ridge (light blue area, solid line). The volume of the open valve up to the circular ridge was also calculated (dotted line). We then predicted the maximum volume trapped for each valve based on

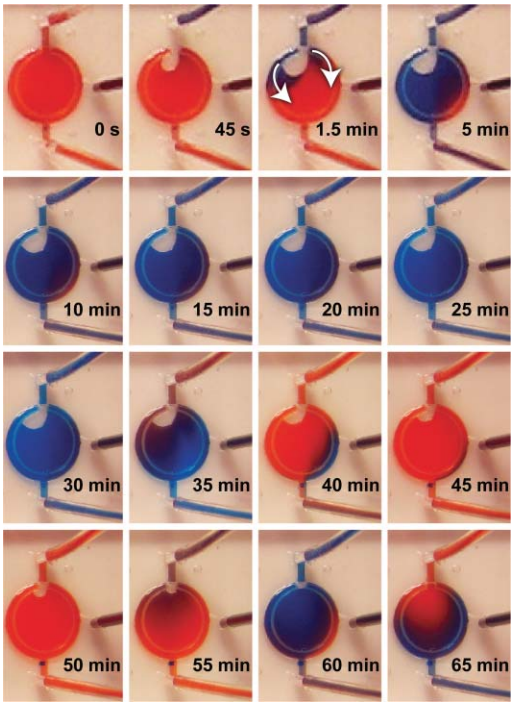

Fig. 3 Timelapse images of the bubble trap and debubbling process. At $t = 0$ s the trap is filled with red solution. At $t = 45$ s the bubble is seen entering the valve, followed by blue solution. At $t = 1.5$ min the bubble is fully inside the valve and immobilized, and the blue solution is able to flow around the bubble through to the fluidic outlet. At $t = 35$ min the bubble has reduced in size, and a further exchange of solution (blue to red) demonstrates that there is still fluid flow through the trapping area. At $t = 55$ min the solution is changed once more (red to blue) and at $t = 65$ min the bubble has finally been removed from the system.

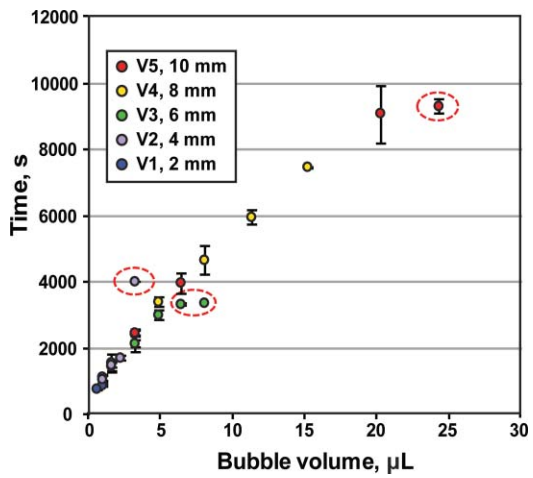

Fig. 4 Bubble removal times for a series of different bubble traps. The time to remove the bubble is linearly dependent on the bubble volume and independent of the trap size. Outlying points, indicated by red circles, demonstrate deviation from the linear relationship due to the bubble extending beyond the circular trap region.

the observed behavior: bubbles would first fill the entire inner circular area, then expand into the channel on one side of the ridge. This calculated volume is shown as the dashed line (inner volume + $\frac{1}{2}$ outer volume), and the experimentally determined volumes are shown as red circles. There is an excellent correlation

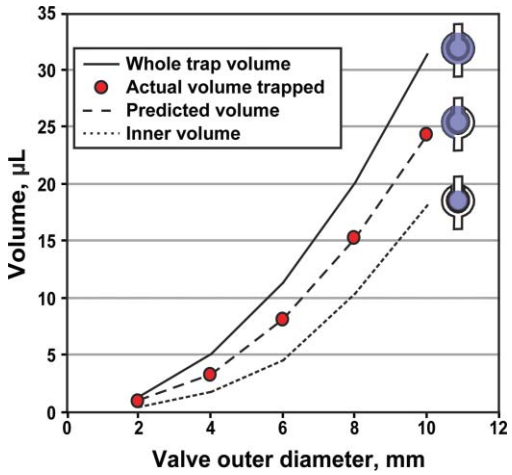

Fig. 5 Calculated and measured maximum trapping volumes. The outer lines show the calculated volumes based on the inner and outer dimensions of the trap. The inner volume plus half the volume of the outer channel (dashes) overlaps precisely with the measured maximum volumes (red circles).

between the predicted and observed values, demonstrating the reproducibility of this trap geometry.

Discussion

We have presented a bubble trap geometry that can both trap and remove bubbles from microfluidic systems during normal operation. The trap is designed to be incorporated directly upstream of bubble-sensitive microfluidic features, and allows normal device operation (*i.e.* steady flow, normal device pressure) to be maintained throughout the trapping and debubbling process. The critical design feature is the thickness of the actuating PDMS membrane: thin membranes (< 250 µm) were found to be difficult to cure and handle, but thicker membranes would result in slower debubbling times. The channel height and ridge width are then chosen based on the desired application: our culture channels were 250 µm tall, which, in combination with a 250 µm thick membrane, set the thickness of the bottom PDMS layer at 500 µm. The ridge height is the same as the channel height, so the ridge thickness must be appropriate ($> 1 : 1$) to ensure it does not collapse when the trap is closed. Finally, the height of the pneumatic chamber is chosen based upon how the device is assembled: we ideally wanted to use this device on both glass and polystyrene, which meant reversible bonding. We had observed delamination when using pneumatic chambers deeper than 150 µm, primarily due to the PDMS membrane stretching and pulling away from the glass or polystyrene bottom. Permanently bonding the PDMS to a glass substrate prevents this behavior, in which case deeper chambers (and potentially less membrane contact with the roof and faster debubbling rates) are possible. We also used a cover plate to clamp the PDMS to polystyrene when plasma bonding was not possible, although the devices will remain attached to untreated surfaces without clamping as long as the applied fluidic pressure remains low.

Using our chosen design parameters, the traps work over a range of sizes, from 2 to 10 mm in diameter, providing a range of designs that can be adapted to different applications. We have demonstrated trapping of bubbles up to 25 µL in volume, and

 This journal is © The Royal Society of Chemistry 2008

can remove these bubbles in under 3 h, all the while keeping continuous, bubble-free flow through the system. We observed a roughly linear relationship between bubble volume and removal time, resulting in a debubbling rate of 0.0023 μL s^{-1}. Based on the steady state flux (dV/dt) across the PDMS membrane we can determine the approximate area that is exposed to vacuum:

$$\frac{dV}{dt} = \frac{AP(p_2 - p_1)}{b} \frac{T}{273} \frac{76}{P_{atm}}$$

where P is the permeability of PDMS (1.92×10^{-15} m^2 s^{-1} Pa^{-1}), p_2 and p_1 are the permeate and feed pressures (here set at net 97 kPa), b is the membrane thickness (250 μm in our devices) and A is the membrane area through which the bubble is removed, P_{atm} is the atmospheric pressure in cmHg, and T is the temperature in Kelvin. Using our above values and our experimentally determined flux we calculate an area of 2.8 mm^2. This value is ~ 2–5× larger than we expect based on our observation of the traps when actuated. It is possible that the permeability used above does not adequately describe the permeability of our membrane when stretched, and also that the membrane thickness is less than 250 μm when in debubbling mode. The flux we observed for our bubble traps is on the order of that observed by Kang *et al.* when pressurizing their devices at 2 psi; they were able to achieve greater debubbling rates but at the expense of added pressure inside the device.[5] We could increase our rates by increasing the height of the pneumatic chamber and limiting the area of PDMS contact, but for our operations these rates are more than acceptable.

The traps we describe here work predictably over a range of geometries and can be potentially integrated into different microfluidic devices. The traps are trivial to add if normally closed PDMS valves are already featured in the device.[6] Using the design constraints described above and based on our experimentally determined debubbling rates, the trap size necessary can be determined by the user to suit their debubbling needs: typical bubbles sizes generated by disconnecting tubing are more on the order of 2 to 5 μL, and as long as only a single bubble is generated per 1 hour period then a 6 mm trap will be suitable to contain and remove this bubble from the system. If larger bubbles are routinely generated, or smaller bubbles are repeatedly generated faster than they can be removed, then a larger trap (8–10 mm) would be necessary.

The debubblers presented here have been incorporated into our perfusion cell-culture microsystems and are routinely used for multi-day experiments.

Acknowledgements

This work was supported by the National Institutes of Health (EB008764).

References

1 L. Kim, Y. C. Toh, J. Voldman and H. Yu, *Lab Chip*, 2007, **7**, 681–694.
2 N. Z. Li and A. Folch, *Exp. Cell Res.*, 2005, **311**, 307–316.
3 L. Kim, M. D. Vahey, H. Y. Lee and J. Voldman, *Lab Chip*, 2006, **6**, 394–406.
4 D. Eddington, *Chips & Tips (Lab on a Chip)*, 22 November 2006, http://www.rsc.org/Publishing/Journals/lc/bubble_trap.asp.
5 J. H. Kang, Y. C. Kim and J. K. Park, *Lab Chip*, 2008, **8**, 176–178.
6 D. Irimia and M. Toner, *Lab Chip*, 2006, **6**, 345–352.